

# A DETERMINATION STUDY OF THE CAVITY EMISSIVITY OF THE EUTECTIC FIXED POINTS CO-C, PT-C AND RE-C

(to be published in International Journal of Thermophysics)

P. Bloembergen<sup>1</sup>, L. M. Hanssen<sup>2</sup>, S. N. Mekhontsev<sup>2</sup>,  
P. Castro<sup>3</sup>, Y. Yamada<sup>4</sup>

<sup>1</sup> *NIM, Beijing, China*

<sup>2</sup> *NIST, Gaithersburg, MD, USA*

<sup>3</sup> *University of Valladolid, Valladolid, Spain*

<sup>4</sup> *NMIJ/AIST, Tsukuba, Japan*

*E-mail (corresponding author): p.bloembergen@xs4all.nl*

## Abstract

The eutectics Co-C, Pt-C and Re-C, with eutectic temperatures of 1597 K, 2011 K, and 2747K, respectively, are presently investigated for their suitability to serve as reference points for dissemination of  $T$  (and  $T_{90}$ ) within the context of the “Mise en pratique of the definition of the Kelvin” (*MeP-K*) at high temperature. Temperatures are to be measured by means of radiation thermometry of cavity radiators imbedded in the associated eutectic. This paper deals with the determination of the respective spectral effective cavity emissivities, which are influenced by the reflective properties of the graphite constituting the cavity on the one hand, and by the temperature distribution within the cavity and over the radiation-shield structure in front of the cavity, on the other. We have begun a comprehensive effort to determine the effective spectral cavity emissivities at 405 nm and 650 nm. The overall program, taking 7 steps in total, involves diverse measurements on representative graphite samples, furnace-temperature profile measurements, calculations of temperature distributions, and, finally, based upon this information, calculation of the cavity-emissivity dependencies. We report here on the current status of the study, including cavity temperature distributions and Monte Carlo modeling results, associated with steps 5, 6 and 7 of the envisaged overall project. For the time being the modeling assumes current estimates of the graphite emissivity and BRDF, which will be updated as data become available from steps 1 to 4.

**Keywords:** Emissivity; Eutectics; High temperatures; Fixed Point; Freezing Point; Blackbody; Monte Carlo Modeling

## 1. Introduction

With the advent of high-temperature eutectics and peritectics with transition temperatures covering the range from 1427 K (Fe-C) to 3458 K (HfC-C) a new era in temperature measurement at high temperature, i.e. above the silver point, will be entered.[1] Under the auspices of WG-5 of the CCT the eutectics Co-C, Pt-C and Re-C, with eutectic temperatures of 1597 K, 2011 K, 2747 K, respectively, are presently investigated for their suitability to serve as reference points for dissemination of  $T$  (and  $T_{90}$ ),[2] within the context of the ‘*Mise en pratique of the definition of the kelvin*’ (MeP-K) at high temperature: MeP-K-HT.[3]

Temperatures are to be measured by means of radiation thermometry of cavity radiators imbedded in the associated eutectic. This paper deals with the determination of the spectral effective cavity emissivities for Co-C, Pt-C and Re-C, which are influenced by the reflective properties of the graphite constituting the cavity on the one hand, and by the temperature distribution within the cavity and over the radiation-shield structure in front of the cavity, on the other.

The envisaged overall program to determining the effective spectral emissivities at 405 nm and 650 nm is shortly reviewed in Section 2. It takes 7 steps in total, involving diverse reflectance measurements on representative graphite samples, furnace-temperature profile measurements, calculations of temperature distributions, and, finally, based upon this information, calculation of the cavity-emissivity dependencies.

Section 3 elaborates on the thermal modeling. Modeling of the various systems considered is done by FLUENT<sup>®</sup>,[4] a software package utilizing *finite-volume* analysis, usually applied in the study of liquids and gases. Furnace-temperature profiles, carried by eight radiation fields placed ahead of the cell are measured by NMIJ at the Co-C, Pt-C and Re-C eutectic fixed points. This has been reported earlier in Reference [5]. The temperature between measured points is then interpolated and the profile is introduced as a contour condition of the model on the external wall of the blackbody tube, eventually allowing the modeling of the cavity temperature distributions.

Section 4 reviews the current status of the project, including cavity temperature distributions and Monte Carlo modeling results, associated with steps 5, 6 and 7 of the envisaged overall

project, reviewed in Section 2. For the time being the modeling assumes current estimates of the graphite emissivity and BRDF, which will be updated as data become available from steps 1 to 4. The calculations are based upon the General Specular Diffuse (GSD) Model involving the directional-hemispherical reflectance  $\rho(\lambda, \theta)$ , made up of a partial diffuse reflectance (PDR) term complemented by a partial reflectance (PSR) term, the latter in Schlick's approximation. Section 5 shows the results obtained thus far; these are discussed in Section 6. Section 7 concludes the paper.

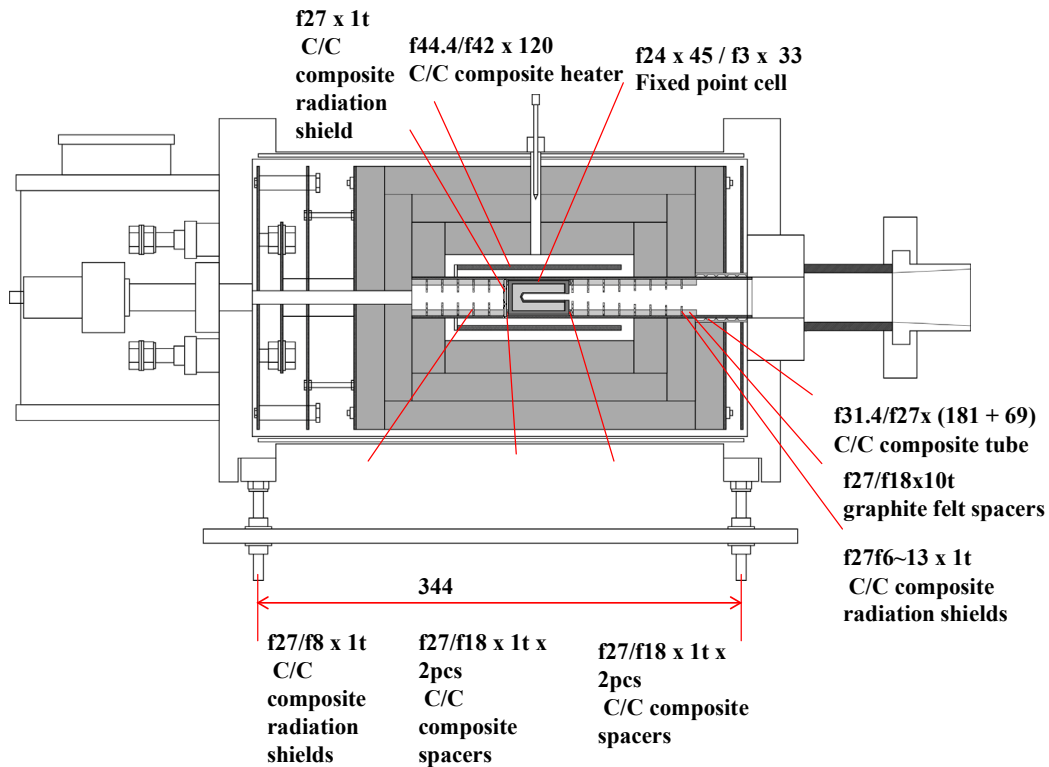


Figure 1. Schematic cross-section view of high temperature furnace with crucible located in the central heating zone.

## 2. Envisaged overall program

The overall program consists of 7 steps:

- (1) Spectral hemispherical reflectance of graphite samples under neutral gas purge at temperatures above ambient (up to a maximum of about 1200 K). This would provide the near-normal directional emittance.
- (2) Full room-temperature bi-directional reflectance distribution function (BRDF) at 405 nm and 650 nm. These measurements can be validated with hemispherical reflectance at the same wavelengths obtained in step 1. At the same time, the BRDF results can validate the restricted BRDF measurement set in step 3.

- (3) Temperature dependent BRDF samples at a few fixed geometries up to 3000 K. Assuming that the relative BRDF angular distribution does not change with temperature, these measurements will allow scaling the reflectance (from step 2), and hence the near-normal emissivity, up to 3000 K.
- (4) Angle-dependent relative spectral radiance at 405 nm and 650 nm under vacuum at temperatures up to 3000 K in the same setup as step 3 to obtain the angle dependent emittance.
- (5) Furnace-temperature profiles of the radiation-shield structure in front of the cavity measured at the eutectic temperatures of the eutectics in study.
- (6) Calculations of the temperature distributions within the cavity and along its outer environment, using a software package utilizing finite volume analysis, with input from step 5.
- (7) Monte Carlo ray-trace modeling of the effective spectral cavity emissivity with input of the results of all steps 1 to 6.

### **3. Thermal modeling**

Modeling of the various systems to be considered is done by FLUENT©[4] a software package utilizing finite-volume analysis, commonly applied to the study of liquids and gases.

Several assumptions were necessary in order to simplify the problem of calculating the parameters in question: 1) the model geometry is considered axisymmetric; this allowed us to construct a 2D model; 2) the thermal resistance at contacting elements or screw parts is neglected because of its relatively small influence and the difficulty of estimating it; 3) heat transfer due to convection and conduction in the furnace atmosphere has been taken into account, but these turned out to be negligible; and 4) the model assumes steady-state conditions.

The thermal conductivity of graphite as a function of temperature over the range of interest, is taken from Reference [6]. From this the values 53.6, 45.6, 36.5 in  $\text{Wm}^{-1}\text{K}^{-1}$  at the fixed point temperatures of the eutectics Co-C(1597 K), Pt-C (2011 K), Re-C (2747 K), respectively, are derived. The emissivity of graphite, quoted nominally as 0.86, is taken from Reference [7].

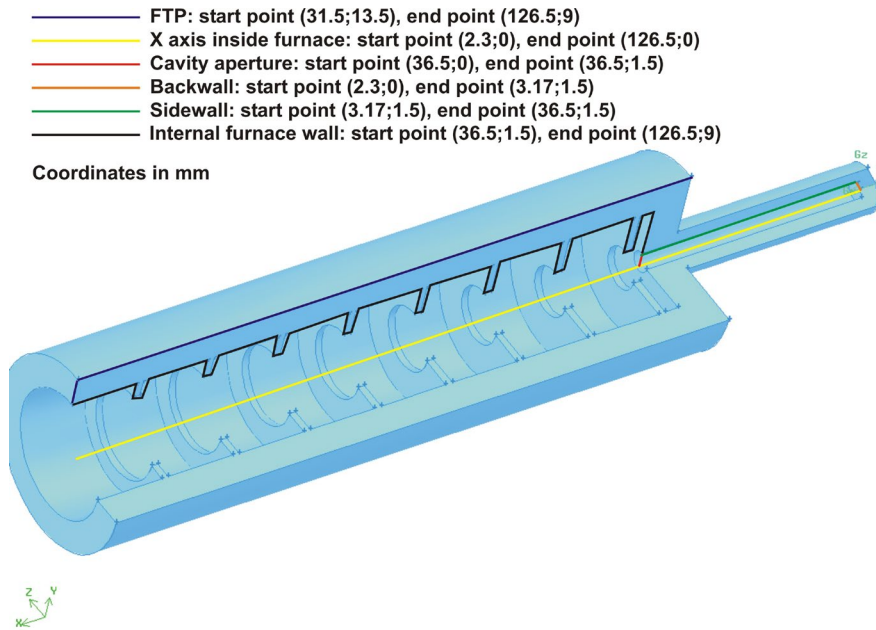


Figure 2. 3D cross-sectional view of the cavity structure including the front furnace baffle structure to present a uniform temperature field to the smaller fixed point crucible section at the right end.

Furnace-temperature profiles, carried by eight radiation fields placed ahead of the cell are measured by NMIJ at the Co-C, Pt-C and Re-C eutectic fixed points. The temperature between measured points is then interpolated and the profile is introduced as a contour condition of the model on the external wall of the blackbody tube. The resulting calculated temperature profiles of the inner walls of the crucible and furnace are shown in Figure 3 (a) and (b) in both absolute and relative terms, respectively. These results are used for the radiance calculations in the next Section.

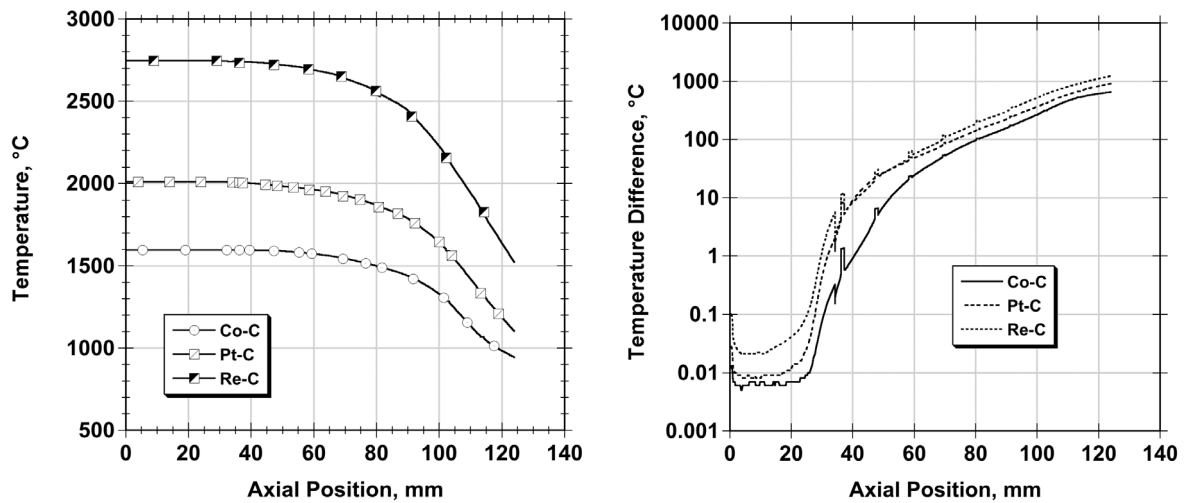


Figure 3. (a) Calculated temperature profiles along the fixed-point crucible and furnace (shown in Figure 2) for the three carbon eutectics. (b) The same profiles shown in terms of the temperature difference relative to the crucible apex temperature.

#### 4. Monte Carlo raytrace analysis model

We have employed a multipurpose custom-developed Monte Carlo raytrace program to perform analysis on the cavity structure shown in Figure 2, with the temperature distribution calculated in Section 3 as input. The paired numbers represent the locations in mm along, and perpendicular to, the primary (X) axis, respectively. The modeling algorithm makes use of reciprocity-based backward ray tracing. It uses the Well Equidistributed Long-period Linear (WELL) pseudorandom number generator.[8] It assumes and incorporates the effects of ambient radiation as isotropic perfectly black background having temperature  $T_{bg}$  (assumed to be 300 K). It can take spectral (wavelength dependent) cavity surface reflectance or emittance as input and can produce spectrally dependent cavity emissivity, radiance and radiance temperature as output.

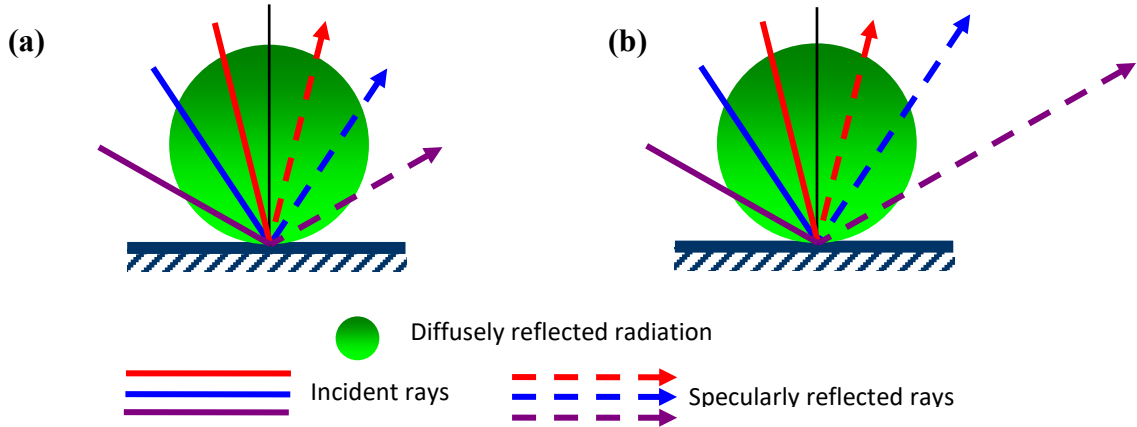


Figure 4. Schematic of the two scattering models used within the Monte Carlo cavity model: (a) the Uniform Specular-Diffuse (USD) model, and (b) the General Specular-Diffuse (GSD) model of reflection.

A schematic comparing the scattering model used for our Monte Carlo cavity model to the simpler more commonly used model, is shown in Figure 4: (a) the Uniform Specular-Diffuse (USD) model, and (b) the General Specular-Diffuse (GSD) model of reflection. The USD is a simple specular-diffuse model widely used in the Monte Carlo modeling of blackbodies (see, e.g. References [9 - 11]), whereas the GSD is a more realistic specular-diffuse model, which takes into consideration the dependence of specular component on incidence angle. The GSD is described by the following equation:

$$\rho(\lambda, \theta_i) = k_d \cdot R_d(\lambda) + (1 - k_d) R_s(\lambda, \theta_i), \quad (1)$$

where

$r(\lambda, \theta)$  is the DHR for wavelength and incidence angle ,

$R_d(\lambda)$  is the partial diffuse reflectance (PDR),

$R_i(\lambda, \theta)$  is the partial specular reflectance (PSR), and

$k_d$  is the weight of diffuse component.

We use Schlick's approximation [11] of Fresnel's law for the PSR at all wavelengths:

$$R_s(\lambda, \theta_i) = R_s(\lambda, 0) + (1 - R_s(\lambda, 0)) (1 - \cos(\theta_i))^5. \quad (2)$$

From the model output, we calculate the effective emissivity estimate using the expression:

$$\varepsilon_e(\lambda, T_{ref}) = \frac{1}{N} \left[ \exp\left(\frac{c_2}{\lambda T_{ref}}\right) - 1 \right]^{-1} \times \sum_{i=1}^N \left\{ \left[ \exp\left(\frac{c_2}{\lambda T_{bg}}\right) - 1 \right]^{-1} \rho^{M_i}(\lambda, \theta_{i, M_j}) + \sum_{j=1}^{M_i} [1 - \rho(\lambda, \theta_{i, j})] \rho^{j-1}(\lambda, \theta_{i, j}) \left[ \exp\left(\frac{c_2}{\lambda T_{i, j}}\right) - 1 \right]^{-1} \right\}, \quad (3)$$

where

$\lambda$  is the wavelength,

$T_{ref}$  is the reference temperature (temperature of cavity bottom center in this case),

$T_{bg}$  is the background temperature,

$c_2$  is the second radiation constant in Planck's law,

$N$  is the number of rays traced,

$M_i$  is the number of reflections of  $i^{\text{th}}$  ray until escaping the cavity,

$\theta_{i, j}$  is the angle of the  $i^{\text{th}}$  ray incidence at the  $j^{\text{th}}$  reflection, and

$T_{bg}$  is the temperature of cavity's wall at the point of the  $j^{\text{th}}$  reflection of the  $i^{\text{th}}$  ray.

The expression for the radiance temperature  $T_s$  is given by:

$$T_s(\lambda) = c_2 \lambda^{-1} \ln \left[ 1 + \frac{\exp\left(\frac{c_2}{\lambda T_{ref}}\right) - 1}{\varepsilon_e(\lambda, T_{ref})} \right]. \quad (4)$$

Given  $10^6$  traced rays, the standard deviation of the effective emissivity for a perfectly diffuse cavity will be less than  $3 \times 10^{-6}$ . For  $10^7$  traced rays, the standard deviation of the effective emissivity for a cavity with the optical properties of its internal surface described by the GSD model, will be approximately  $2 \times 10^{-5}$ .

## 5. Monte Carlo raytrace results.

Since the actual emittance, reflectance and scattering character of the graphite surface in the crucibles and furnaces during operation are not well known at this point in the study, we have

chosen to examine the modeled system with a range of the key parameters of emittance and the weight of the diffuse component. In Figures 5 (a) and (c), the radiance temperatures of the Co-C and Re-C crucibles are shown for the wavelengths of interest (405 nm and 650 nm), for the isothermal and Lambertian graphite case. Results are shown for graphite emittance values of 0.7 and 0.8, as well as 1.0 (to show the ideal blackbody case for comparison). In Figures 5 (b) and (d), the effective emissivities corresponding to (a) and (b), respectively, are shown, as well as those for the non-isothermal case, with temperature distributions taken from the profiles shown in Figure 3. The effects of non-Lambertian reflectance of the graphite are examined in Figure 6, using the GSD model of reflectance described in Section 4, for Co-C and Re-C cavities. The radiance temperature, shown in (a) and (c), and the effective emissivity shown in (b) and (d), are plotted versus the diffuse component weight,  $k_d$ .

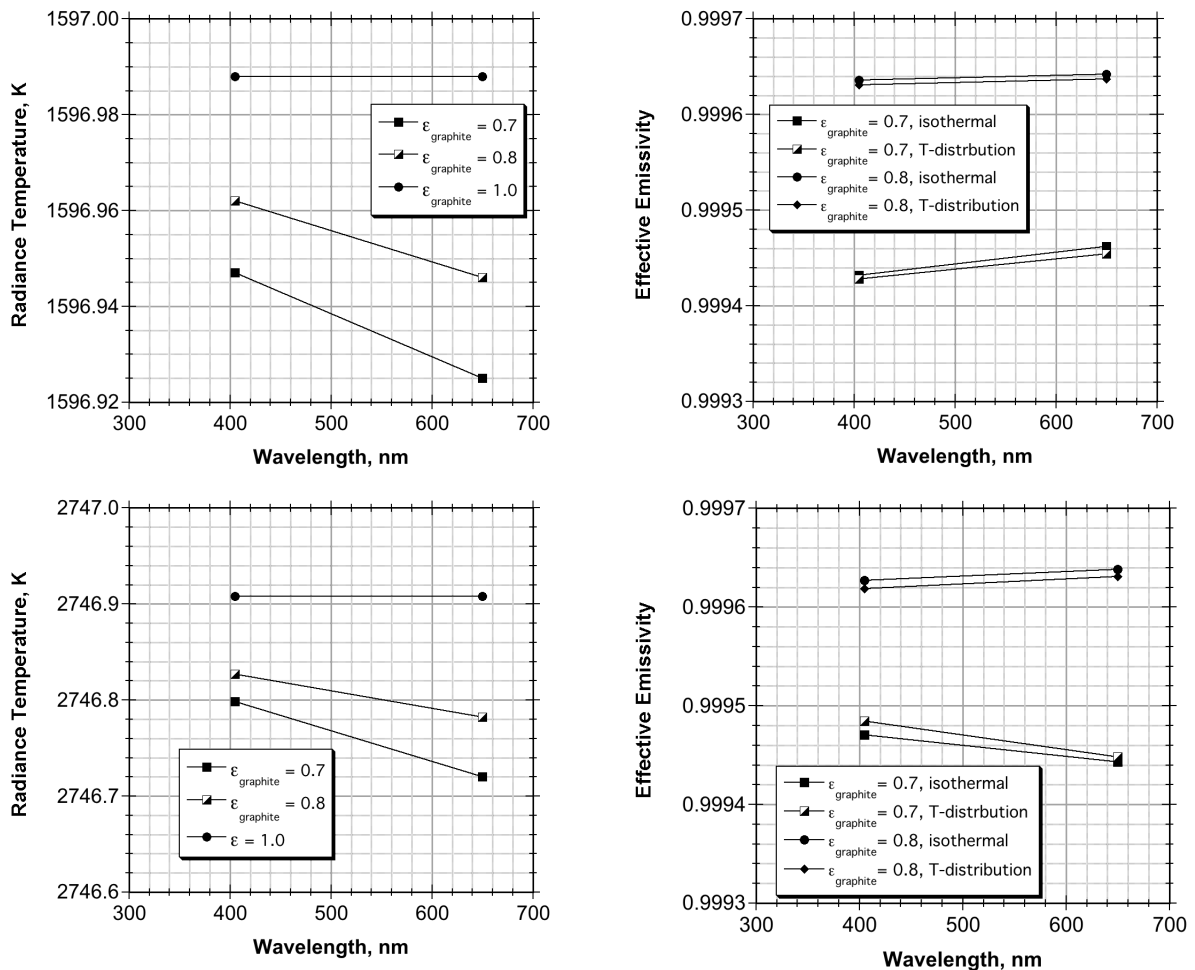


Figure 5. Radiance temperature (a, c) and graphite emittance and wavelength, as the graphite fixed point cavities near the d). The right hand plots include data for both temperature distributions calculated by

effective emissivity (b, d) dependence on determined from Monte Carlo simulations of melting points of Co-C (a, b) and Re-C (c, isothermal cavities as well as for ones with thermal modeling and shown in Figure 2.



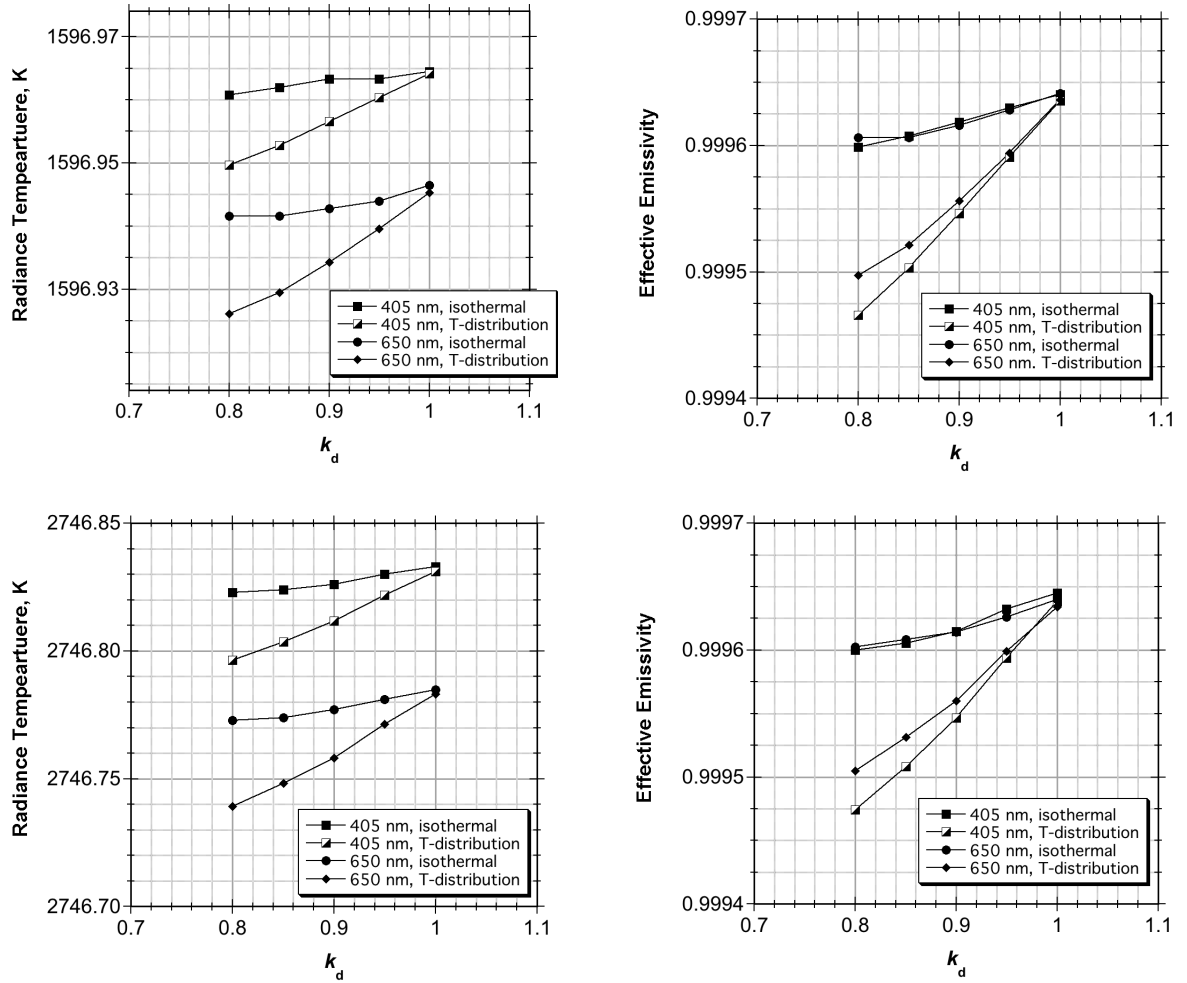


Figure 6. Radiance temperature (a, c) and effective emissivity (b, d) dependence on graphite diffusivity and wavelength, as determined from Monte Carlo simulations of the graphite fixed point cavities near the melting points of Co-C (a, b) and Re-C (c, d). Data are shown for both the isothermal and non-isothermal cases (according to the temperature distributions from Figure 2).

For the Lambertian graphite case, as seen in Figure 5 (b) and (d), there is almost no effect of the calculated non-isothermal temperature distributions on the cavity emissivities. Conversely, the results show that the furnace design would be a sufficient approximation to isothermality, provided the graphite reflectance is Lambertian. On the other hand, as can be seen in the results shown in Figure 6 (a – d), the existence of a specular component of the graphite reflectance leads to a slight decrease of the radiance temperature and cavity effective emissivity, but when a specular component is coupled with the non-uniform temperature distribution, the decrease becomes potentially significant (a change of  $10^{-4}$  in effective emissivity and 10 to 35 mK in radiance temperature for a  $k_d$  of 0.8).

## **6. Summary and conclusions.**

We are in the midst of an effort to establish effective emissivity values with minimal uncertainties for fixed-point blackbody cavities using the eutectics Co-C, Pt-C and Re-C. We have studied, by measurement and modeling, the temperature distribution within one cavity design optimized for and presently employed in the operation of existing eutectic blackbodies.[5] The temperature distributions, have, in turn, been used as input data to a custom Monte-Carlo-based ray tracing code to examine the potential variability of the cavity effective emissivity due to the temperature distributions and the graphite reflectance characteristics. Simulating the graphite reflectance by a combination of a Lambertian component and an angle dependent specular component, the modeling results indicate that the combination of a specular component together with a realistic non-uniform cavity temperature can result in a modest change in the cavity effective emissivity.

Although the graphite reflectance model is only an approximation of the actual BRDF, we expect the trends described in this paper to qualitatively represent those of an actual cavity. For more quantitative (accurate) results, we will be measuring the graphite BRDF and upgrading the Monte Carlo code to incorporate the BRDF data in future steps of our planned program.

## **Acknowledgement.**

The authors would like to thank Alexander Prokhorov for his valuable contributions in developing and customizing the Monte Carlo raytracing code, based on the STEEP 3 Program Series from Virial Inc.[4]

## References

1. Y. Yamada, “Advances in High-Temperature Standards above 1000 °C”, MAPAN **20**, No. 2, 183-191 (2005).
2. G. Machin, P. Bloembergen, J. Hartmann, M. Sadli, Y. Yamada, “A concerted international project to establish high temperature fixed points for primary thermometry”, Int. J. Thermophys. **28**, 1976-1982 (2007)
3. “Mise en pratique for the definition of the kelvin”  
[http://www.bipm.org/utls/en/pdf/MeP\\_K.pdf](http://www.bipm.org/utls/en/pdf/MeP_K.pdf)
4. Certain commercial equipment, instruments, or materials are identified in this paper to specify the experimental procedure adequately. Such identification is not intended to imply recommendation or endorsement by the National Institute of Standards and Technology, nor is it intended to imply that the materials or equipment identified are necessarily the best available for the purpose.
5. P. Castro, P. Bloembergen, Y. Yamada, M.A. Villamanan, G. Machin, “On the uncertainty in the Temperature Drop across the Backwall of High-Temperature Fixed Points”, Acta Metrologica Sinica **29**, 253 – 260 (2008).
6. Y. S. Touloukian, R. W. Poweel, C. Y. Ho, P. G. Klemens, “Thermal conductivity: Nonmetallic Solids, Thermophysical Properties of Matter,” The TPRCX Data Series **2**, New York, Plenum Press, 1978.
7. J. Fischer, H. J. Jung, “Determination of the thermodynamic temperatures of the freezing points of silver and gold by near-infrared pyrometry, Metrologia **26**, 245-252 (1989).
8. P. L'Ecuyer, F. Panneton, M. Matsumoto, “Improved Long-Period Generators Based on Linear Recurrences Modulo 2,” ACM Transactions on Mathematical Software **32**, No. 1, 1–16 (2006).
9. A. Ono, “Calculation of the Directional Emissivities of the Cavities by the Monte Carlo Method,” J. Opt. Soc. Am. **70**, 547-554 (1980).

10. V. I. Sapritsky and A. V. Prokhorov, "Calculation of the Effective Emissivities of Specular- Diffuse Cavities by the Monte Carlo Method," *Metrologia* **29**, 9-14 (1992).
11. Alexander V Prokhorov and Leonard M Hanssen, "Effective emissivity of a cylindrical cavity with an inclined bottom: II. Non-isothermal cavity," *Metrologia* **46** 1–14 (2009)
12. Schlick C., "An inexpensive BRDF model for physically-based rendering," *Computer Graphics Forum (Proc. Eurographics '94)* **13**, No. 3, 233-246 (1994).